Environ Geol (2008) 54:291–308
DOI 10.1007/s00254-007-0817-4

ORIGINAL ARTICLE

Hydrogeological and hydrogeochemical characterization of a karstic mountain region

Celalettin Simsek · Alper Elci · Orhan Gunduz · Burhan Erdogan

Received: 2 March 2007 / Accepted: 15 May 2007 / Published online: 19 June 2007

Abstract Karstic limestone formations in the Mediterranean basin are potential water resources that can meet a significant portion of groundwater demand. Therefore, it is necessary to thoroughly study the hydrogeology and hydrogeochemistry of karstic mountain regions. This paper presents a detailed hydrogeological and hydrogeochemical characterization of the Nif Mountain karstic aquifer system in western Turkey, an important recharge source for the densely populated surrounding area. Based on the geological and hydrogeological studies, four major aquifers were identified in the study area including the allochthonous limestone in Bornova flysch, conglomerate-sandstone and clayey-limestone in Neogene series, and the Quaternary alluvium. Physicochemical characteristics of groundwater were measured in situ, and samples were collected at 59 locations comprised of springs and wells. Samples were analyzed for major ions, isotopic composition, arsenic, boron and heavy metals among other trace elements. It was found that the hydrogeological structure is complex with many springs having a wide range of discharge rates. High-discharge springs originate from allochthonous limestone units, whereas low-discharge springs are formed at the contacts with claystone and limestone units. Using stable isotope analysis data, a δ^{18}O-deuterium relationship was obtained that lies between the Mediterranean meteoric and mean global lines. Tritium analyses showed that low-discharge springs originating from contact zones had longer circulation times compared to the high-discharge karstic springs. Furthermore, hydrogeochemical data revealed that groundwater quality significantly deteriorated as water moved from the mountain to the plains. Heavy metal, arsenic and boron concentrations were generally within drinking-water quality standards with a few exceptions occurring in residential and industrial areas located at the foothills of the mountain. Elevated arsenic concentrations were related to local geologic formations, which are likely to contain oxidized sulfite minerals in claystones. It is concluded that Nif Mountain overall has a significant potential to provide high-quality water with a safe yield of at least 50 million m^3/year, which corresponds to about 28% of the mean annual inflow to the Tahtali reservoir, a major water resource for the city of Izmir.

Keywords Allochthonous karstic aquifer · Hydrogeology · Isotopic composition · Water quality · Nif Mountain, Turkey

C. Simsek (✉)
Department of Drilling,
Torbali Technical Vocational School of Higher Education,
Dokuz Eylul University, 35860 Torbali-Izmir, Turkey
e-mail: celalettin@deu.edu.tr

A. Elci · O. Gunduz
Department of Environmental Engineering,
Dokuz Eylul University, 35160 Buca-Izmir, Turkey
e-mail: alper.elci@deu.edu.tr

O. Gunduz
e-mail: orhan.gunduz@deu.edu.tr

B. Erdogan
Department of Geological Engineering,
Dokuz Eylul University, 35160 Buca-Izmir, Turkey
e-mail: burhan.erdogan@deu.edu.tr

Introduction

Karst aquifers are known to be difficult to comprehend due to their unique geological and hydrogeological features. Nevertheless, these aquifer systems meet a significant portion of groundwater demand worldwide (Hiscock 2005).

The water supply potential of karst aquifers is mainly determined by the regional precipitation amount, the permeability of limestone formations, the tectonic structure, and the inherent discontinuities (i.e., fault lines, fractures, joints, layering) of the geological structure. Depending on the saturated groundwater flux in limestone formations, karstic structures such as caves, dolines, channels and uvala form during the flow and dissolution process (Sen 1995). Consequently, the permeability of karst aquifers arises primarily from the enlargement of joints and bedding plane partings as limestone is dissolved by circulating groundwater (White 2002).

The hydrogeological properties of karst aquifers are determined by the geology of the region of interest and the geomorphologic properties of the surrounding area. In general, the circulation of groundwater in karst aquifers is quite different from water circulation in nonkarstic aquifers (Kacaroglu 1999). Karst aquifers also provide more favorable conditions for groundwater recharge as compared to other aquifer types. Surface water flow to karst medium is more rapid compared to granular aquifers allowing much more rapid replenishment of groundwater. On the other hand, this hydrogeological characteristic of karst systems is also responsible for the fast movement of pollutants originating from surface sources, thus making these systems more vulnerable to surface contamination.

From a structural point view, karst systems might be classified into two major groups: (1) massive carbonate platforms and (2) allochthonous limestone formations. The massive carbonate rocks are generally characterized by their well-defined stratigraphy and large spatial extent, whereas allochthonous limestone formations are typically distinguished by their deformed geology and limited spatial extent. In many areas, the allochthonous limestones are observed nonuniformly inside flysch units that are mainly comprised of meta-sandstone, shale and ophiolites, which complicates the identification of their hydrogeological structure. These limestone units shape major karstic formations and are known to have significant water potential. In general, the discharge and recharge mechanisms of allochthonous limestone units demonstrate diverse characteristics since some of these units are totally buried inside the impervious flysch formation, whereas others are partially covered and reach the surface in many locations. Furthermore, the presence of different rocks with variable chemical compositions around these limestones influences the quality of groundwater originating from such karstic units.

In Turkey, limestone formations are predominantly encountered in the Aegean region and along the Mediterranean coastline within the Taurus Mountain range. Generally in the Aegean region and particularly around Izmir, the limestone formations are, for the most part, allochthonous in nature. They vary in size ranging from a few hundred meters up to 20 km inside flysch units (Erdogan and Gungor 1992). Within the immediate vicinity of the city of Izmir, these allochthonous limestone formations are observed at the highest elevation of Nif Mountain, i.e., up to 1,400 m. In addition, these units are observed to have thickness values ranging as high as 200 m. The formations are predominantly comprised of Upper Cretaceous-aged limestone platforms and are regarded as the most significant karstic rock of the region. As they are primarily surrounded by flysch formations around the Izmir area, these units in and around Nif Mountain are typically of an allochthonous nature.

Because the surrounding flysch formations are considerably less permeable, the karst aquifer system that is recharged from Nif Mountain is considered to be an important groundwater resource in the region. In this regard, Nif Mountain hosts a number of large springs with discharge rates exceeding 100 L/s. The majority of these springs reach the surface in locations where the highly permeable allochthonous limestone interfaces with flysch formations. The flysch formations in Nif Mountain are intermingled with meta-sandstone, shale, ophiolite and serpantinite units. The complex nature of the regional geology influences the hydrogeological properties as well as the geochemical composition of water that flows through them.

This study is intended to characterize the hydrogeology and the hydrogeochemistry of the Nif Mountain karstic aquifer system. With a total drainage area of more than 1,000 km^2, the Nif Mountain karstic aquifer system is considered to be an important unit of the domestic water supply system of the city of Izmir, the third largest metropolitan area of Turkey. Furthermore, the karstic structure in Nif Mountain recharges the surrounding Bornova, Kemalpasa and Torbali plains, where intense agricultural and industrial production takes place, as well as the Cumaovasi plain where the Tahtali Dam Reservoir of the Izmir water supply system is situated. In this regard, the quality of subsurface drainage originating from Nif Mountain is considered to be an important factor that determines the overall water quality pattern around the Izmir metropolitan area.

Description of study area

The study area is located to the southeast of the city of Izmir, which is on the Aegean coast in western Turkey (Fig. 1). From a geomorphological point of view, the study area mainly consists of Nif Mountain and the surrounding plains. The selected study area is delineated such that Nif Mountain is situated at the center and a number of low

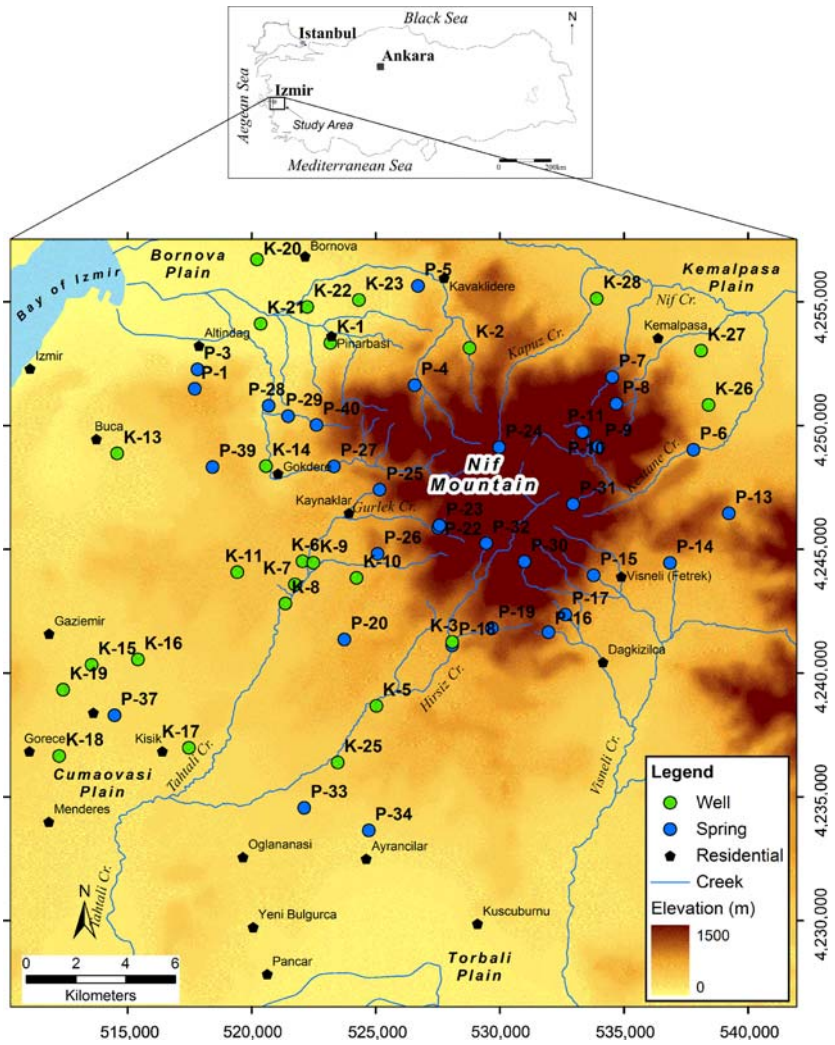

Fig. 1 Map of the study area and sampling points

level plains in all directions surround the mountain. In particular, the northern parts of the area are characterized by graben fault lines directed E-W (<15 km) that have shaped the surrounding plains in the area (Inci 1991). Thus, the northern parts of Nif Mountain are characterized by extreme slopes merging into the Kemalpasa and Bornova plains. On the other hand, the slopes on the western and eastern sides of the mountain are milder. Numerous deep fault systems in varying directions are observed in many parts of the study area where allochthonous limestone units are present. In particular, these deep fault systems are encountered in the vicinity of the mountain summit, where slopes are greater compared to lower elevations (Fig. 1).

The study area of slightly more than 1,000 km^2 is located in a region that demonstrates typical characteristics of the Mediterranean climate with mild, rainy winters and hot, dry summers. Based on the data collected at the Bornova Meteorological Station between 1979 and 2005, the region receives a mean annual precipitation of 594 mm. The highest precipitation amounts are observed in November, December and January, with long-term monthly averages of 100, 120 and 106 mm, respectively. The lowest precipitation values are observed in July and August with long-term monthly averages of 2.3 and 1.8 mm, respectively (DMI 2006). During winter months, the precipitation typically occurs in the form of snow around the summit of Nif Mountain (1,450 m), but no permanent snow cover occurs due to moderate temperatures with a mean above 0°C.

Being situated within the administrative boundaries of the third largest city and in the vicinity of one of the most industrialized areas of Turkey, Nif Mountain is under immense environmental stresses due to residential, agricultural and industrial development. In particular, the fertile agricultural plains are being converted to organized industrial zones and/or residential lots in Bornova, Cumaovasi, Kemalpasa and Torbali plains. This transformation is the main reason for the increase in population density in the region. In addition to the city of Izmir, Bornova, Kemalpasa, Buca, Menderes and Torbali are

among the major counties of Izmir that are situated around Nif Mountain. According to the 2000 census data, about 850,000 inhabitants live within these counties at the lower elevations of Nif Mountain. The population density decreases with proximity to Nif Mountain, on which only a few small villages exist on the hillslopes.

Geological setting

Based on the regional geology shown in Fig. 2 and the cross-sectional view given in Fig. 3, four different rock types are observed in and around the study area: (1) the Paleozoic-aged Menderes metamorphics, which mainly consist of schists, (2) the Mesozoic-aged Bornova flysch, which mostly contains meta-sandstones, shales, ophiolites as well as the Upper Cretaceous-aged allochthonous limestones, (3) the Neogene-aged conglomerates, claystones, and clayey-limestones, which are collectively known as the Visneli Formation, and (4) the Quaternary-aged alluviums. Of these units, the Menderes metamorphics are considered to be the foundation rock, on which Bornova flysch lies nonuniformly via a thrust fault. In general, Menderes metamorphics are observed mainly as schists with limited spatial extent in eastern parts of the study area. The Bornova flysch, including the allochthonous limestones, is the main rock type of the Nif Mountain area as shown in Figs. 2 and 3. The western and southern portions of the mountain are mostly characterized by the Neogene series including conglomerates, sandstones, claystones, and limestones. Finally, the northern and southwestern parts of the study area are mostly covered by alluvial layers.

The local geology of Nif Mountain is mainly characterized by the Mesozoic-aged Bornova flysch, which is comprised of sandstones, shales, clays and ophiolites as well as variably sized allochthonous limestones (Figs. 2 and 3). Bornova flysch is a common formation around Izmir and demonstrates a rather heterogeneous matrix of complex geology. One of the most distinctive characteristics of Bornova flysch is the presence of variably sized allochthonous limestones within its matrix structure. These allochthonous limestone units are blocks that separated from a large limestone structure (i.e., Karaburun Carbonate Platform) located to the west of Izmir and fell into the flysch unit during the early stages of its development (Erdogan and Gungor 1992). It is reported that the size of these limestones might reach up to 20 km and could demonstrate similar structural and tectonic characteristics to the Upper Cretaceous-aged Karaburun

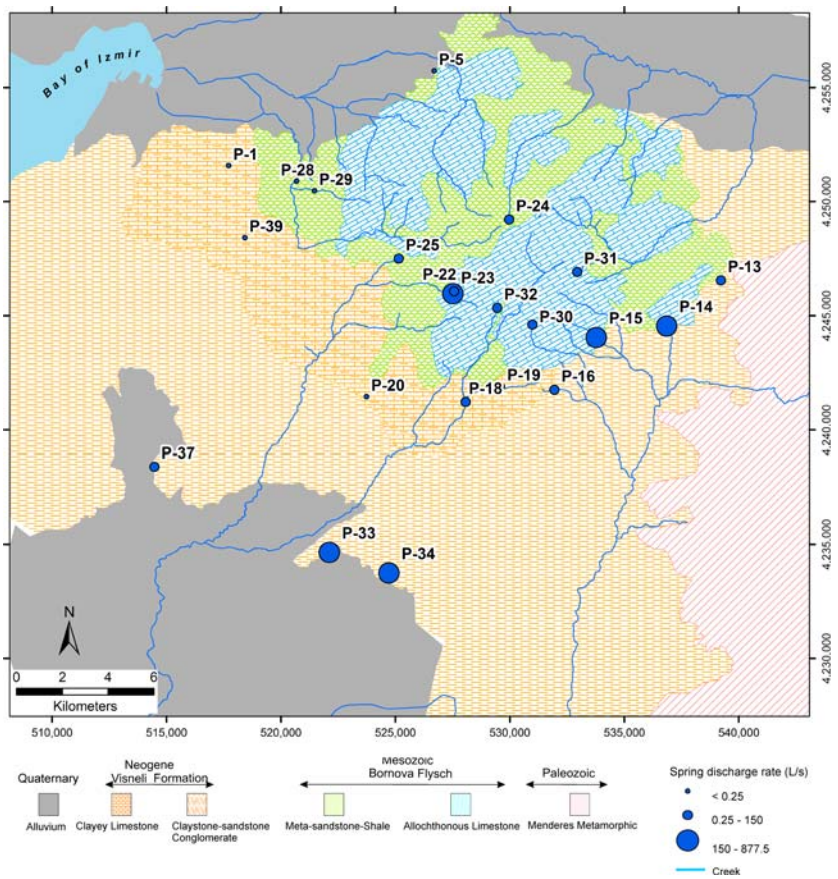

Fig. 2 Geological map of the study area with discharge rates of major springs

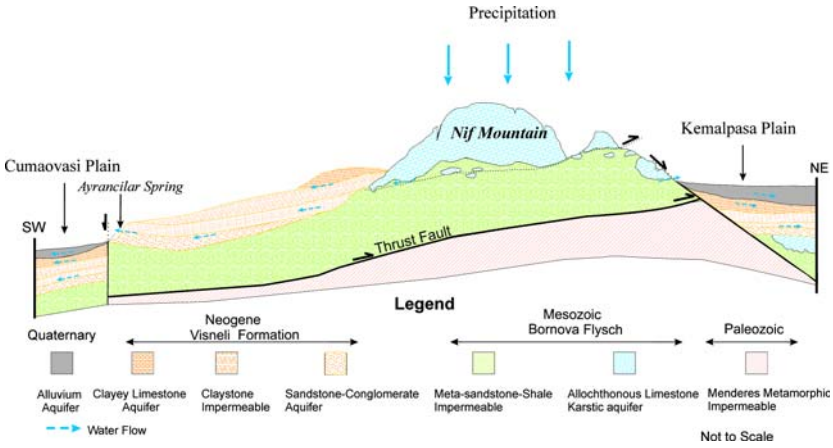

Fig. 3 Conceptual hydrogeological cross-section of the study area

Carbonate Platform (Erdogan and Gungor 1992). Within the study area, these limestone units are typically found at high elevations and display an extremely fractured pattern. The water movement inside these units is dominated by caves, faults and cracks that occur as a result of fault lines directed NW-SE and NE-SW. The cracks directed NE-SW are deeper and are responsible for the general NE-SW direction of the surface drainage pattern in the study area.

When the general stratigraphy of the study area was further analyzed, it could be seen that the Neogene-aged series lie nonuniformly over the Bornova flysch. These Neogene-aged series are collectively named the Visneli Formation in the Nif Mountain area. The Visneli Formation mainly consists of a number of rocks including but not limited to conglomerates, sandstones, claystones, and clayey limestones (Baba and Sozbilir 2001). This formation is widely observed in the southern and southwestern parts of the study area. Finally, the Quaternary-aged alluvial layers overlie the Bornova flysch and Visneli Formation in the region. The thickness of the alluvial layer ranges from 40–120 m in the Bornova and Kemalpasa plains and from 20–80 m in the Torbali and Cumaovasi plains (Simsek 2002; Demirkiran et al. 2006).

From a tectonic point of view, the study area is located in the Alpine-Himalayan orogenic belt and is a part of a tectonically active zone with numerous fault lines (Sozbilir 2000). The major tectonic footprints observed in the study area are the graben faults directed E-W with lengths ranging up to 15 km, which are cut by secondary cracks directed N-S (Inci 1991). These graben faults formed several graben plains including the Bornova and Kemalpasa plains located in the north and northeast of the study area, respectively. These vertical fault systems control the formation and the thickness of the alluvial layers that develop on the surface of the plains. Moreover, they also influence the aquifer properties of the alluvial layers such that the surface waters draining from upper elevations of Nif Mountain seep into the alluvial layers and form regional groundwater aquifer systems inside the plains.

Materials and methods

The characterization of the Nif karst aquifer system is a two-stage process that involves (1) field work and (2) sample analysis. The field work was conducted as a series of field excursions for the general assessment of regional geology and hydrogeology where in situ measurements of several water quality parameters were done, samples were collected for laboratory analysis, and geological characterization of the regional morphology was conducted. The sample analyses, on the other hand, were performed in several national and international laboratories for a complete description of the regional hydrogeology.

Field work

The project field work was conducted as a series of expeditions to Nif Mountain and its vicinity in 2005 and 2006. This stage was initiated with a preliminary field exploration that was conducted with the aid of a 1/25,000 scaled topographic basemap and a handheld GPS device. During this exploration, potential sampling locations within the study area (i.e., natural springs and accessible wells screened in the unconfined aquifer) were designated and marked on the basemap. The type of sampling location (well or spring) and its spatial coordinates (X, Y, Z) were recorded. Several other additional details were also noted such as the depth and the average production capacity in cases of wells, and the mechanism of water outflow and discharge rate in cases of springs. The database was then shortlisted to a total of 59 sampling points by considering the spatial distribution of the points within the general study area and by taking into account the particular significance of the point for the project's objectives. The data

collected from the field work were then transferred into a database that was hosted by a GIS platform for spatial analysis and data visualization. The selected 59 data points (25 wells and 34 springs) were later revisited in several other field trips for sample collection and further analysis.

During the field trips, the geology of the study area was delineated by field observations and was complemented by a regional geology map obtained from the General Directorate of Mineral Research and Exploration (MTA). In addition to the particular points of interest from a hydrogeological point of view, the field surveys also focused on a number of geological features including but not limited to faults, fractures, layer slopes and bearings. These features were measured, recorded, and drawn on the map.

The water quality sampling was performed during the field studies conducted in April and May of 2006, which roughly marked the end of the wet period of the year. Some basic physicochemical parameters such as pH, electrical conductivity, water temperature and salinity were measured in situ with portable multiparameter probes. For other parameters of interest, water samples were collected into 50-, 500- and 1,000-mL polyethylene bottles from each sampling location. These bottles were temporarily stored in portable coolers and were then transferred to constant-temperature refrigeration units located in the Water Quality Laboratories of Dokuz Eylul University at the end of each sampling day for further hydrogeochemical analysis.

Sample analyses

The water samples collected from 59 sampling points were analyzed for major anions and cations, heavy metals and trace elements. The 50-mL sample collected from each point was acidified in the field with nitric acid to drop the pH level below 2. This pretreated sample was then analyzed by inductively coupled plasma mass spectrometry (ICP-MS) for major cations and several trace elements such as arsenic, boron and iron at Canadian ACME Laboratories. The 500-mL sample collected from each sampling point was used to analyze major anions such as chloride, bromide, nitrate, nitrite, fluoride, sulfate and bicarbonate ions. Of these, only the bicarbonate analysis was performed by titrimetric techniques; the remaining anions were analyzed by ion chromatography (IC) in Dokuz Eylul University laboratories. Finally, the 1,000-mL samples collected from 14 selected karstic springs were tested for stable isotopes $\delta^{18}O$ (oxygen-18), $\delta^{2}H$ (deuterium), and $\delta^{3}H$ (tritium) in the isotope laboratories of Hacettepe University, Turkey, and University of California, USA. The oxygen-18 and deuterium analyses were performed using a Finnigan MAT 251 Isotope Ratio Mass Spectrometer, and the tritium analysis was done using a liquid scintillation counter.

Results and discussion

This section presents the results of this study with regard to the hydrological and hydrogeological characteristics, isotopic composition, and hydrogeochemical properties of the Nif Mountain karstic aquifer system. The entire characterization was performed using data collected from 59 sampling points (25 wells and 34 springs), each of which has some interaction with the karstic system under consideration (Fig. 1). In the following paragraphs, the hydrology and hydrogeology of Nif Mountain and its vicinity are presented with particular emphasis on the natural springs and wells based on a series of field excursions. Then, the isotopic composition of some major springs is described to characterize the recharge and circulation mechanisms of the Nif karstic aquifer system. Finally, a hydrogeochemical characterization of the 59 data points is made to depict the overall chemical status of water originating from Nif Mountain with respect to drinking water quality. The results are presented in Tables 1, 2, and 3.

Hydrological and hydrogeological characteristics

A wide network of streams and creeks has developed in and around the vicinity of Nif Mountain as seen in Fig. 1. Among the most important of these streams, the perennial Hirsiz and Gurlek creeks originate from the southwestern slopes of the mountain and later merge to form the Tahtali stream, which flows through the heavily populated Cumaovasi plain. The Tahtali stream is the major tributary of the Tahtali reservoir that was constructed in the 1990s to serve the water supply needs of the Izmir metropolitan area. The Kapuz and Kestane creeks originate from the northeastern slopes of the mountain and later merge to form the Nif stream, which flows into the industrialized Kemalpasa plain before merging with the Gediz River. Finally, the Visneli stream originates from the southeastern slopes of the mountain and is mainly fed by two karstic springs (P-14 and P-15). The Visneli stream flows into the Torbali plain, which is considered to be an important agricultural production area and an industrial development region. With long-term mean daily flow values of less than 10 m^3/s, the Tahtali, Nif, and Visneli streams are important recharge sources for their corresponding underlying surficial aquifers.

In addition to the surface drainage network mentioned above, the study area also has a well-developed subsurface system of aquifers. A total of four major aquifer units have been detected in the area: (1) the allochthonous karstic limestones located within the flysch units, (2) the conglomerate and sandstone units of the Visneli Formation, (3) the clayey limestone units of the Visneli Formation, and (4)

Table 1 Isotopic composition of some sampled springs

Spring no.	*X* (m)	*Y* (m)	*Z* (m)	Discharge rate (L/s)	T (°C)	pH	EC (μS/cm)	$\delta^{18}O$ (‰)	$\delta^{2}H$ (‰)	$\delta^{2}H$ excess (%)	Tritium (TU)
P-4	526,781.8	4,251,761.3	369	NA	12.8	7.76	351	–6.36	–34.2	6.67	4.40
P-6	537,800.4	4,249,025.0	273	NA	16.6	7.33	467	–6.62	–35.7	7.23	4.58
P-7	534,532.2	4,251,955.4	650	NA	12.0	7.60	328	–7.15	–39.8	7.41	3.90
P-9	533,970.9	4,249,150.5	861	NA	10.8	7.80	237	–7.14	–39.9	7.22	4.05
P-10	533,402.1	4,249,728.4	954	NA	11.2	7.87	215	–7.47	–42.5	7.29	4.82
P-14	536,854.5	4,244,450.9	320	256.00	16.3	7.10	612	–6.92	–38.1	7.32	4.70
P-15	533,778.2	4,243,949.5	421	185.00	14.1	7.18	371	–7.11	–38.4	8.49	4.21
P-18	528,073.8	4,241,121.9	361	0.67	14.7	6.93	586	–5.82	–32.0	4.53	3.27
P-22	527,515.4	4,245,869.2	619	NA	11.9	7.74	258	–7.47	–41.8	7.92	4.17
P-27	523,314.6	4,248,350.3	279	NA	13.4	7.25	516	–5.95	–33.6	3.98	4.71
P-29	521,466.6	4,250,378.3	144	0.07	15.4	6.62	891	–5.49	–29.8	4.10	4.46
P-30	530,990.5	4,244,508.0	1,027	0.49	12.4	7.28	511	–6.79	–35.5	8.87	3.51
P-31	532,945.9	4,246,821.9	1,116	1.25	10.7	7.93	212	–7.60	–42.5	8.30	3.96
P-33	522,115.8	4,234,555.4	138	NA	17.3	6.59	497	–6.84	–38.5	6.18	3.27
P-34	524,717.0	4,233,647.5	103	877.50	17.3	7.13	574	–6.73	–37.3	6.53	4.01

NA Not available (could not be measured)

the alluvium layers (Figs. 2, 3). Among these formations, the clayey limestones of the Visneli Formation and the surficial alluvial layers demonstrate unconfined aquifer characteristics. The conglomerates and sandstones of the Visneli Formation are considered to represent confined aquifer characteristics in many locations of the study area as these units are mostly overlaid with clay and clayey-limestone units. The allochthonous limestones of the flysch units, on the other hand, exhibit a dual character, such that some portions of these rocks located in the Kemalpasa and Bornova plains are considered to be a confined aquifer, whereas other portions in the study area could be regarded as an unconfined aquifer.

A detailed assessment of the regional geology and the above-mentioned aquifer systems reveals that the most important water-bearing unit in the study area is the allochthonous karstic limestone aquifer. The Neogene series (conglomerate-sandstone and clayey-limestone) aquifers and Quaternary alluvial aquifer systems are in general of secondary importance for the region, as they have a relatively lower water supply potential compared to the karstic limestone units. In this regard, wells that are drilled in the allochthonous limestone units have been proven to provide significant amounts of water (i.e., as high as 50 L/s from a typical well depth of less than 300 m). It must also be mentioned that all of these aquifer systems are recharged by Nif Mountain via infiltration from surface runoff and horizontal seepage from subsurface interflow.

During the field excursions, it was verified that numerous wells have been drilled in and around the Nif Mountain area for water supply purposes. Furthermore, the majority of these wells are located below an elevation of 300 m, particularly in lowland areas such as the Bornova, Kemalpasa, Torbali, and Cumaovasi plains. These wells are typically drilled in the alluvial, the Neogene conglomerate, and the limestone aquifers. Although the depths of these wells are rather variable depending on the aquifer system into which they are drilled, wells dug in the alluvial aquifers are generally shallower than 100 m. Based on the logs collected from several boreholes, the average thicknesses of the alluvial layers are between 40 and 80 m in the Bornova plain and between 20 and 60 m in the Kemalpasa plain. Both plains are typically characterized as coarse-grained sands and gravels, from which about 10 L/s discharge could be realized from wells ranging between 50 and 80 m in depth. However, the overexploitation of the alluvial aquifers in these plains has created significant drawdowns in water levels, which in turn has resulted in the construction of deeper wells that penetrate the underlying conglomerate and limestone aquifers. Particularly in the Bornova and Kemalpasa plains, the wells drilled in these formations range between 120 and 250 m in depth. For industries that require vast amounts of water (i.e., beverage and brewery industries), wells are drilled in the alloctonous limestone units with depths exceeding 350 m in the Bornova and Kemalpasa plains. The specific yield of these wells has previously been determined to be greater than 30 L s^{-1} m^{-1} as discussed by Demirkiran et al. (2006). It must also be noted that there are a few exceptionally deep wells (i.e., 750 m and more) drilled in the allochthonous limestone units of the Kemalpasa plain, which were discovered as a result of detailed geophysical surveys.

Table 2 Physicochemical characteristics of groundwater samples

Sample point	Spatial coordinates			General parameters				Major cations				Major anions						Major trace elements							
	X (m)	*Y* (m)	*Z* (m)	*T* (°C)	pH	EC (μS/cm)	$CaCO_3$ (mg/L)	Ca (mg/L)	Mg (mg/L)	Na (mg/L)	K (mg/L)	HCO_3 (mg/L)	Fl (mg/L)	Cl (mg/L)	Br (mg/L)	NO_3 (mg/L)	SO_4 (mg/L)	Al (μg/L)	As (μg/L)	B (μg/L)	Cu (μg/L)	Fe (μg/L)	Li (μg/L)	Mn (μg/L)	Zn (μg/L)
K-1	523,170.6	4,253,339.7	59	16.1	7.31	562	334.90	108.33	15.71	11.04	1.13	355	0.10	17.61	0.22	11.96	16.82	1.0	0.8	20.0	1.4	<10.0	2.8	0.1	29.1
K-2	528,776.4	4,253,136.0	280	14.5	7.29	495	310.50	97.47	16.37	6.84	0.56	393.8	0.10	8.88	0.24	0.48	10.29	14.0	5.2	9.0	2.9	14.0	3.3	0.6	13.8
K-3	528,082.0	4,241,260.0	388	16.0	7.01	643	409.20	108.78	31.56	9.28	1.72	448	0.07	12.53	0.25	15.49	21.17	<1	34.1	24.0	1.2	<10.0	2.4	0.7	19.7
K-5	525,025.5	4,238,673.3	250	18.1	6.61	941	538.50	182.69	20.11	22.33	3.00	577	0.09	57.71	0.31	23.00	30.34	1.0	3.8	61.0	1.3	<10.0	19.5	4.3	2,992.4
K-6	522,050.3	4,244,518.6	212	17.2	7.10	663	395.00	135.48	13.86	13.14	1.85	438.7	0.25	22.87	0.28	10.05	14.38	5.0	1.2	22.0	3.9	<10.0	10.9	1.6	1,312.4
K-7	521,742.7	4,243,583.9	205	17.0	7.42	811	143.40	30.96	16.08	167.31	5.44	589	0.24	6.72	0.34	0.39	2.09	2.0	4.6	727.0	52.3	<10.0	147.6	4.8	1,618.4
K-8	521,355.7	4,242,810.3	191	14.8	7.22	765	569.40	128.42	36.22	14.00	2.75	494	0.36	25.94	0.29	18.96	57.74	1.0	254.4	44.0	2.4	<10.0	39.2	0.9	55.8
K-9	522,485.1	4,244,456.0	244	17.3	7.00	781	427.70	162.53	16.34	13.92	0.64	462.3	0.60	30.43	0.30	35.10	41.09	11.0	<0.5	19.0	0.5	<10.0	5.2	3.9	5.3
K-10	524,227.1	4,243,844.9	279	16.1	7.05	669	398.30	117.03	25.84	16.62	1.32	400	0.48	18.46	0.28	21.20	25.55	6.0	<0.5	26.0	2.5	434.0	5.6	3.7	103.1
K-11	519,419.6	4,244,075.3	246	21.3	7.37	654	231.70	41.71	30.52	66.63	22.07	428.9	0.92	28.39	0.30	0.19	14.52	2.0	463.3	498.0	0.5	29.0	943.1	32.4	52.6
K-13	514,580.3	4,248,873.4	78	19.2	7.30	880	453.30	155.66	15.77	32.42	3.77	437.9	0.31	42.63	0.29	41.13	13.77	7.0	15.4	234.0	12.7	<10.0	47.6	0.5	569.1
K-14	520,575.3	4,248,363.7	173	14.3	7.30	896	434.90	113.86	36.66	54.97	1.21	450.1	0.62	48.31	0.35	0.30	58.82	49.0	0.7	137.0	1.5	50.0	67.0	4.3	26.2
K-15	513,555.1	4,240,337.9	131	19.4	6.98	631	354.20	117.12	15.07	20.96	1.35	451.6	0.68	28.10	0.28	2.87	6.20	36.0	9.5	107.0	2.2	55.0	40.7	14.5	3.9
K-16	515,415.6	4,240,549.5	148	17.8	6.85	758	445.10	162.92	9.38	13.26	1.29	493.8	0.56	25.75	0.28	21.80	5.54	3.0	9.1	64.0	4.2	17.0	25.4	0.7	8.1
K-17	517,469.5	4,236,984.1	139	19.0	7.03	632	384.60	128.06	15.82	11.48	0.93	420.4	0.18	17.03	0.28	16.00	6.02	4.0	3.2	36.0	1.5	<10.0	19.3	0.7	128.0
K-18	512,247.3	4,236,651.1	135	17.0	6.46	1,318	519.90	133.96	45.13	89.79	6.14	312	0.21	152.20	0.43	164.20	89.92	449.0	2.3	85.0	2.9	333.0	16.7	16.0	284.9
K-19	512,404.6	4,239,330.6	130	22.6	7.84	776	28.20	9.87	0.88	195.21	2.70	407.2	0.38	54.61	0.49	0.50	16.82	<1	8.2	909.0	0.1	<10.0	364.7	27.3	<0.5
K-20	520,216.1	4,256,708.8	42	18.5	6.96	681	371.80	121.34	16.80	21.25	2.06	401.6	0.55	30.31	0.33	22.72	12.99	<1	7.1	70.0	0.4	27.0	20.6	5.8	92.0
K-21	520,358.8	4,254,113.4	43	16.4	7.17	743	432.40	138.54	21.08	18.70	1.23	420	0.65	42.82	0.27	18.33	24.86	2.0	<0.5	23.0	1.5	<10.0	2.8	0.3	2.4
K-22	522,239.7	4,254,792.9	58	18.8	7.35	1,228	426.90	126.57	27.00	120.54	1.38	374.5	0.69	174.39	0.30	38.31	39.65	5.0	1.0	88.0	0.7	12.0	3.8	0.6	5.8
K-23	524,322.0	4,255,072.6	94	21.1	7.28	592	354.00	107.17	21.05	12.80	1.54	392.5	1.22	19.98	0.26	10.92	22.13	1.0	15.5	49.0	3.5	<10.0	6.3	0.5	49.1
K-25	526,082.5	4,254,373.1	140	15.8	7.11	815	409.00	139.07	15.07	16.89	0.97	412	0.17	18.25	0.31	44.30	15.61	7.0	0.9	19.0	0.7	68.0	2.6	1.8	<0.5
K-26	538,403.5	4,250,833.5	252	13.0	7.20	486	300.70	92.25	17.15	7.44	1.51	347.5	0.07	9.16	0.24	3.75	14.73	1.0	3.8	13.0	0.9	27.0	2.3	0.5	33.2
K-27	538,103.3	4,253,022.9	173	17.6	6.84	774	446.50	156.96	13.34	20.26	3.23	485.8	0.15	27.32	0.27	27.52	28.91	9.0	0.6	34.0	2.2	143.0	2.8	2.1	148.8
K-28	533,901.0	4,255,130.2	218	15.6	7.10	628	382.40	128.17	15.23	10.52	1.37	406	0.46	26.91	0.26	16.19	14.48	3.0	1.5	15.0	1.1	40.0	3.5	1.5	67.5
P-1	517,710.7	4,251,486.2	268	14.4	7.93	448	260.60	99.99	2.71	8.82	0.57	215.6	0.49	17.29	0.29	17.65	57.38	7.0	4.3	27.0	0.6	<10.0	1.6	0.6	1.4
P-3	517,817.1	4,252,270.4	116	17.8	7.43	1,583	640.80	238.99	10.81	98.67	7.02	333.5	0.58	148.45	0.27	293.84	85.09	5.0	2.2	154.0	1.0	27.0	4.7	0.5	1.2
P-4	526,781.8	4,251,761.3	369	12.8	7.76	351	195.90	69.76	5.32	8.56	0.66	193.7	0.51	22.83	0.26	0.23	22.32	26.0	<0.5	12.0	1.4	22.0	0.5	1.2	8.6
P-5	526,702.6	4,255,641.4	194	14.2	6.77	1,042	662.80	247.99	10.71	18.28	0.68	719	0.32	33.49	0.32	0.24	33.43	5.0	<0.5	17.0	1.0	31.0	16.3	1.9	1.1
P-6	537,800.4	4,249,025.0	273	16.6	7.33	467	292.70	92.26	15.21	5.58	0.47	308.6	0.07	8.25	0.24	1.14	8.50	2.0	1.6	10.0	0.6	22.0	1.5	0.5	1.3
P-7	534,532.2	4,251,955.4	650	12.0	7.60	328	196.50	74.04	2.87	3.67	0.54	224.6	0.05	5.65	<0.05	0.44	7.91	6.0	<0.5	6.0	0.3	23.0	0.3	0.3	0.7
P-8	534,687.6	4,250,879.7	801	11.4	7.68	304	188.80	65.84	5.97	3.17	0.66	219.6	0.04	4.29	0.23	0.51	6.72	3.0	<0.5	6.0	0.6	16.0	0.1	0.4	0.8

Table 2 continued

Sample point	Spatial coordinates			General parameters				Major cations				Major anions						Major trace elements							
	X (m)	*Y* (m)	*Z* (m)	*T* (°C)	pH	EC (μS/cm)	$CaCO_3$ (mg/L)	Ca (mg/L)	Mg (mg/L)	Na (mg/L)	K (mg/L)	HCO_3 (mg/L)	Fl (mg/L)	Cl (mg/L)	Br (mg/L)	NO_3 (mg/L)	SO_4 (mg/L)	Al (μg/L)	As (μg/L)	B (μg/L)	Cu (μg/L)	Fe (μg/L)	Li (μg/L)	Mn (μg/L)	Zn (μg/L)
P-9	533,970.9	4,249,150.5	861	10.8	7.80	237	137.60	42.69	7.56	3.76	0.95	167.3	0.05	5.16	0.23	1.04	7.09	13.0	<0.5	6.0	1.5	12.0	0.2	1.6	4.9
P-10	533,402.1	4,249,728.4	954	11.2	7.87	215	126.50	44.64	3.69	3.21	0.65	146.4	0.04	4.61	0.24	1.05	5.68	15.0	<0.5	5.0	0.8	20.0	0.1	2.4	2.2
P-11	533,326.0	4,249,740.3	990	11.5	7.93	216	122.30	43.00	3.65	2.51	0.29	133	0.04	4.35	0.23	1.23	5.40	4.0	<0.5	<5.0	0.4	<10.0	<0.1	0.2	0.8
P-13	539,224.9	4,246,452.4	401	14.7	7.20	675	425.40	113.41	34.62	7.93	0.62	485.6	0.09	12.89	0.25	1.05	16.80	1.0	<0.5	22.0	0.4	<10.0	2.1	3.6	0.7
P-14	536,854.5	4,244,450.9	320	16.3	7.10	612	383.50	104.00	30.15	7.64	0.82	442.6	0.11	13.23	0.25	2.35	16.65	5.0	0.5	11.0	0.4	<10.0	2.6	0.2	1.8
P-15	533,778.2	4,243,949.5	421	14.1	7.18	371	228.10	78.44	7.86	3.88	0.29	236	0.05	6.90	0.24	1.86	6.17	1.0	0.5	6.0	0.3	172.0	0.3	4.1	<0.5
P-16	531,953.2	4,241,654.2	515	15.5	7.07	704	456.40	129.15	32.61	7.45	0.38	505.5	0.07	13.62	0.25	0.36	15.90	<1	<0.5	7.0	0.9	14.0	0.3	0.3	0.8
P-17	532,639.4	4,242,360.4	420	14.8	7.62	333	188.60	57.77	10.81	4.58	0.41	201.6	0.05	8.54	0.24	0.86	8.80	11.0	1.1	7.0	0.8	34.0	0.6	0.9	2.1
P-18	528,073.8	4,241,121.9	361	14.7	6.93	586	363.90	102.78	26.14	6.98	0.96	400	0.07	10.54	0.25	22.14	19.62	2.0	0.6	15.0	1.5	13.0	2.8	0.3	2.3
P-19	529,676.2	4,241,815.0	485	12.3	7.05	859	535.00	139.83	45.74	11.74	0.75	605.3	0.14	29.10	0.26	0.29	25.22	<1	1.4	14.0	0.8	<10.0	3.2	0.9	<0.5
P-20	523,737.4	4,241,355.7	313	15.5	6.94	730	445.90	163.13	9.45	13.18	0.31	457.2	0.11	24.83	0.29	12.11	24.84	4.0	<0.5	19.0	1.3	<10.0	4.5	1.0	2.8
P-22	527,515.4	4,245,869.2	619	11.9	7.74	258	155.80	50.63	7.17	3.22	0.31	200	0.05	5.01	0.24	1.92	6.10	8.0	<0.5	5.0	0.5	10.0	0.1	0.6	17.6
P-23	527,568.2	4,245,969.2	653	11.8	7.50	375	232.60	61.36	19.33	3.97	0.52	264.9	0.07	6.90	0.25	1.87	9.98	13.0	0.8	7.0	1.6	26.0	1.2	6.2	68.1
P-24	529,968.4	4,249,117.3	1102	8.7	7.61	460	276.50	95.14	9.60	4.26	0.56	335.5	0.07	6.43	0.24	0.27	11.43	12.0	0.6	7.0	1.2	14.0	3.0	1.8	84.1
P-25	525,151.6	4,247,406.2	523	14.0	7.65	460	279.30	80.70	19.10	6.73	0.61	335.7	0.06	11.46	0.25	0.55	12.38	9.0	<0.5	9.0	3.5	24.0	1.0	0.9	25.0
P-26	525,075.6	4,244,818.0	413	15.6	6.93	656	418.90	94.01	44.80	7.85	0.59	509.9	0.07	14.67	0.26	0.41	18.55	1.0	<0.5	8.0	0.4	<10.0	1.1	3.6	1.6
P-27	523,314.6	4,248,350.3	279	13.4	7.25	516	310.60	101.54	13.93	7.89	0.59	347.7	0.07	12.87	0.25	0.71	17.06	64.0	<0.5	11.0	0.6	34.0	3.4	0.6	8.1
P-28	520,687.0	4,250,801.0	103	15.9	6.92	889	442.90	125.30	31.66	54.61	1.12	585	0.35	38.57	0.31	0.91	48.87	<1	<0.5	61.0	0.3	14.0	87.2	11.5	0.7
P-29	521,466.6	4,250,378.3	144	15.4	6.62	891	557.20	204.58	11.36	17.11	0.90	598.2	0.09	20.89	0.31	1.10	48.26	6.0	<0.5	17.0	0.7	<10.0	17.2	0.6	1.6
P-30	530,990.5	4,244,508.0	1027	12.4	7.28	511	321.50	103.82	15.19	6.64	0.74	380.8	0.08	11.71	0.24	1.35	13.61	11.0	<0.5	9.0	1.8	33.0	2.6	1.2	3.7
P-31	532,945.9	4,246,821.9	1116	10.7	7.93	212	122.00	38.68	6.19	3.39	0.35	138.6	0.05	5.03	0.24	0.61	9.94	7.0	<0.5	5.0	2.1	10.0	0.1	0.9	4.0
P-32	529,447.8	4,245,245.2	884	13.2	7.65	366	214.10	66.55	11.69	6.21	0.38	218.4	0.05	11.45	0.24	0.73	13.45	6.0	<0.5	7.0	0.7	22.0	0.9	1.1	1.1
P-33	522,115.8	4,234,555.4	138	17.3	6.59	497	284.40	86.46	18.85	5.68	0.60	337.6	0.08	8.73	0.25	4.53	10.14	15.0	4.8	9.0	0.6	45.0	2.2	2.6	1.4
P-34	524,717.0	4,233,647.5	103	17.3	7.13	574	281.20	81.67	18.82	5.61	0.51	316.2	0.07	8.91	0.25	3.82	9.22	4.0	3.5	8.0	0.4	<10.0	1.9	0.4	1.1
P-37	514,473.5	4,238,298.8	163	17.7	7.10	633	371.00	134.39	8.69	9.44	2.32	337.6	0.81	23.25	0.27	32.51	18.96	36.0	6.8	30.0	1.0	39.0	19.8	0.8	1.8
P-39	518,424.0	4,248,325.0	230	17.3	7.48	823	496.00	77.42	73.62	17.70	2.79	627.3	1.33	27.50	0.29	2.94	17.84	2.0	293.8	124.0	0.7	<10.0	764.1	0.2	1.8
P-40	522,613.0	4,250,025.0	274	14.4	7.18	699	438.40	144.99	18.64	12.86	0.70	493	0.48	15.10	0.26	0.34	24.38	11.0	<0.5	22.0	0.8	<10.0	11.7	7.1	2.6

K Well, *P* spring

Table 3 Statistical summary and comparison with drinking water quality criteria

	Unit	Drinking water standard, TSE266[a]	Drinking water standard, EPA[b]	Wells (n = 25)				Springs (n = 34)			
				Max	Min	Mean	SD	Max	Min	Mean	SD
T	°C	25	–	22.60	13.00	17.38	2.29	17.80	8.70	14.05	2.33
pH	–	6.5 < pH < 9.2	6.5 < pH < 8.5	7.84	6.46	7.13	0.28	7.93	6.59	7.35	0.39
EC	μS/cm	2,000	–	1,318.00	486.00	752.88	195.11	1,583.00	212.00	555.32	285.00
$CaCO_3$	mg/L	–	–	569.40	28.20	380.10	116.08	662.80	122.00	325.11	148.23
Ca	mg/L	200	–	182.69	9.87	117.80	40.53	247.99	38.68	101.62	51.49
Mg	mg/L	50	–	45.13	0.88	20.32	9.67	73.62	2.71	17.49	15.19
Na	mg/L	175	–	195.21	6.84	39.50	50.97	98.67	2.51	11.55	17.89
K	mg/L	12	–	22.07	0.56	2.85	4.24	7.02	0.29	0.90	1.20
HCO_3	mg/L	–	–	589.00	312.00	431.98	63.22	719.00	133.00	353.57	159.02
Fl	mg/L	1.5	4.0	1.22	0.07	0.40	0.29	1.33	0.04	0.20	0.28
Cl	mg/L	600	250	174.39	6.72	37.89	40.20	148.45	4.29	17.72	24.76
Br	mg/L	–	–	0.49	0.22	0.30	0.06	0.32	0.05	0.25	0.04
NO_3	mg/L	50	44.3	164.20	0.19	22.63	32.33	293.84	0.23	12.15	50.27
SO_4	mg/L	250	250	89.92	2.09	24.18	20.12	85.09	5.40	19.52	17.19
Al	μg/L	200	200	449.00	1.00	24.88	89.08	64.00	1.00	9.35	12.17
As	μg/L	50	10	463.30	0.50	33.91	102.60	293.80	0.50	9.78	50.21
B	μg/L	2000	–	909.00	9.00	133.32	231.10	154.00	5.00	20.24	32.19
Cu	μg/L	3000	1300	52.30	0.10	4.20	10.32	3.50	0.30	0.93	0.65
Fe	μg/L	200	300	434.00	10.00	54.76	104.20	172.00	10.00	23.15	28.12
Li	μg/L	–	–	943.10	2.30	72.23	196.44	764.10	0.10	28.21	130.92
Mn	μg/L	50	50	32.40	0.10	5.20	8.47	11.50	0.20	1.79	2.39
Zn	μg/L	5000	5000	2992.40	0.50	304.90	690.74	84.10	0.50	7.61	18.20

[a] Maximum allowable concentration

[b] Maximum contaminant level

In the Cumaovasi plain in the Tahtali Basin, the Neogene-aged conglomerates and clayey-limestone units are the major aquifers that are exploited for water supply purposes. In particularly, the wells drilled in the Neogene-aged limestone units with depths ranging between 60 and 300 m could provide discharge rates up to 15 L/s. These Neogene-aged clayey-limestone units range between 20 and 40 m in thickness based on several borehole logs. The alluvial aquifer in the Cumaovasi plain, on the other hand, is limited in total thickness with values ranging between 15 and 30 m, and thus, is generally used for water supply on a temporary basis. Consequently, it is generally utilized for individual uses and small-scale agricultural irrigation. Users requiring large amounts of water generally drill wells in the Neogene-aged limestone units. On the contrary, the wells located in the Torbali plain, situated in the south of the study area, are mostly drilled in the comparatively thick alluvial aquifer that locally reaches up to 80 m in thickness. The alluvial layer in the Torbali plain consists of coarse materials, and the wells in Torbali generally range between 50 and 250 m providing discharges between 15 and 30 L/s.

The complex geological structure and the aquifer formations in the Nif Mountain area and its vicinity resulted in the formation of numerous natural springs. These springs can be classified into four major categories depending on the parent rock, the formation mechanism, and the rate of discharge: (1) high-discharge springs that emerge from the outcropping fractures and cracks in allochthonous limestone units, (2) high-discharge springs that emerge from the surface outcrops of conglomerate and sandstone units of the Visneli Formation, (3) medium- to low-discharge springs that are formed at the contact zones of allochthonous limestone and flysch units, and (4) low-discharge springs that are formed at the contact zones of claystone and clayey-limestone units of the Visneli Formation.

The high-discharge springs originating from allochthonous limestone units have discharge rates higher than 50 L/s, which can sometimes reach up to 300 L/s depending on the annual precipitation pattern. Typical examples of this category are the Visneli (P-14 and P-15) and Gurlek (P-22) springs located in the southeast and west of the study area, respectively. The springs with high-discharge rates emerging from the conglomerates and sandstone units have

discharges in excess of 200 L/s. The seasonal discharge in these locations could occasionally reach up to 1,000 L/s during winter and spring seasons when recharge rates are at maximum. These springs usually have larger recharge areas and are observed at lower elevations of the study area. The Oglananasi (P-33) and Ayrancilar (P-34) springs are considered to be typical examples of this category.

On the other hand, low-discharge springs originating from the contact zones of Neogene-aged claystone and clayey-limestone units typically have discharge rates less than 1 L/s. The springs in the Altindag (P-1) and Kiriklar (P-18) region of the study area belong to this category. Finally, the medium- to low-discharge springs that emerge from the contact zones of allochthonous limestone and flysch units have discharge rates that differ considerably and are generally higher than 1 L/s but typically less than 10 L/s. The rate depends on the spatial extent of the limestone interface at the contact zone. Typical examples of this category are Sekeroluk (P-24) and Esoluk (P-32) springs located in the central portions of the study area. Based on this classification, Fig. 2 shows the distribution of measured discharge rates, demonstrating that major springs (i.e., >50 L/s) are concentrated mostly on the southern and southwestern slopes of Nif Mountain. The springs in the north and northwestern portions of the study area have significantly lower discharge rates (i.e., 0.05–1.25 L/s) based on the measurements conducted in spring 2006.

The State Hydraulics Works (DSI) has monitored discharge rates of major springs in the region since 1985. From the monitoring records, it was observed that a major spring located to the northwest of Nif Mountain in Pinarbasi region started to dry up during summer months beginning in the mid-1990s, due to extensive aquifer exploitation as a result of rapid industrial development in the area. To investigate the relationship between precipitation input and discharge rate of the springs, the hydrographs of three major springs (Oglananasi: P-33, Ayrancilar: P-34, and Pinarbasi: P-41) are compared with storm hydrographs for the wet and dry seasons of the year, shown in Fig. 4a and b, respectively. The wet season corresponds to a period between the months November and April, and the dry season covers a period between the months May and October. From the comparison of hydrographs, one could comment that these springs are mainly fed by storm water and that there is a correlation between their discharge rates and the corresponding precipitation rates.

Isotopic characteristics

A subset of karstic and contact springs was also sampled for isotopic characterization of the Nif Mountain karstic aquifer system. The results of the isotope analyses are presented in Table 1. Based on these results, it can be seen that the $\delta^{18}O$ values range from –7.60 to –5.49‰ and the deuterium $\delta^{2}H$ values range from –42.5 to –29.8‰. In this regard, the values for all water samples lie between the mean global ($\delta^{2}H = 8\delta^{18}O + 10$) and the Mediterranean meteoric lines ($\delta^{2}H = 8 \times \delta^{18}O + 22$) as shown in Fig. 5. A correlation analysis was performed and the following relationship was obtained between $\delta^{18}O$ and $\delta^{2}H$ values for the Nif Mountain karstic aquifer system (designated as Izmir coastline in Fig. 5):

$$\delta^{2}H = 5.94\delta^{18}O + 2.86 \quad (1)$$

It should be noted that this relationship is similar to the data fit for the Antalya station that is given by (IAEA 2002):

$$\delta^{2}H = 6.52\delta^{18}O + 6.78 \quad (2)$$

Although the city of Antalya is geographically located along the Mediterranean Sea coastline in southern Turkey, the relationship obtained in this study (Eq. 1) was quite similar to the data fit for the Antalya station given in Eq. (2). This finding implies that precipitation in both locations occurs under similar climatic conditions. In a comparable study conducted in central Anatolia (Gunay 2006), it was shown that the isotopic composition of groundwater in a karstic aquifer was much closer to the mean global meteoric line than to the relationship found in this study. The relationship between $\delta^{18}O$ and $\delta^{2}H$ in spring water from the karst aquifer in central Anatolia is given by the following equation (Gunay 2006):

$$\delta^{2}H = 8.0\delta^{18}O + 14.5 \quad (3)$$

The differences between these studies could be explained by the drastic differences in the climatic conditions of the central Anatolian and Aegean/Mediterranean regions. Even if two karstic aquifers have similar hydrogeological characteristics, the differences in recharge mechanisms and climatic conditions would ultimately yield distinct isotopic compositions as shown above.

In another study conducted on the Syrian coast, Charideh and Rahman (2006) found the following relationship between deuterium and oxygen-18:

$$\delta^{2}H = 6.0\delta^{18}O + 4.6 \quad (4)$$

This relationship is similar to Eq. (2) that was written for Antalya station, thus implying a representative relationship for the eastern Mediterranean Sea.

In addition to the correlation between oxygen-18 and deuterium, the excess deuterium ($\%d = \delta^{2}H–8.0 \times \delta^{18}O$)

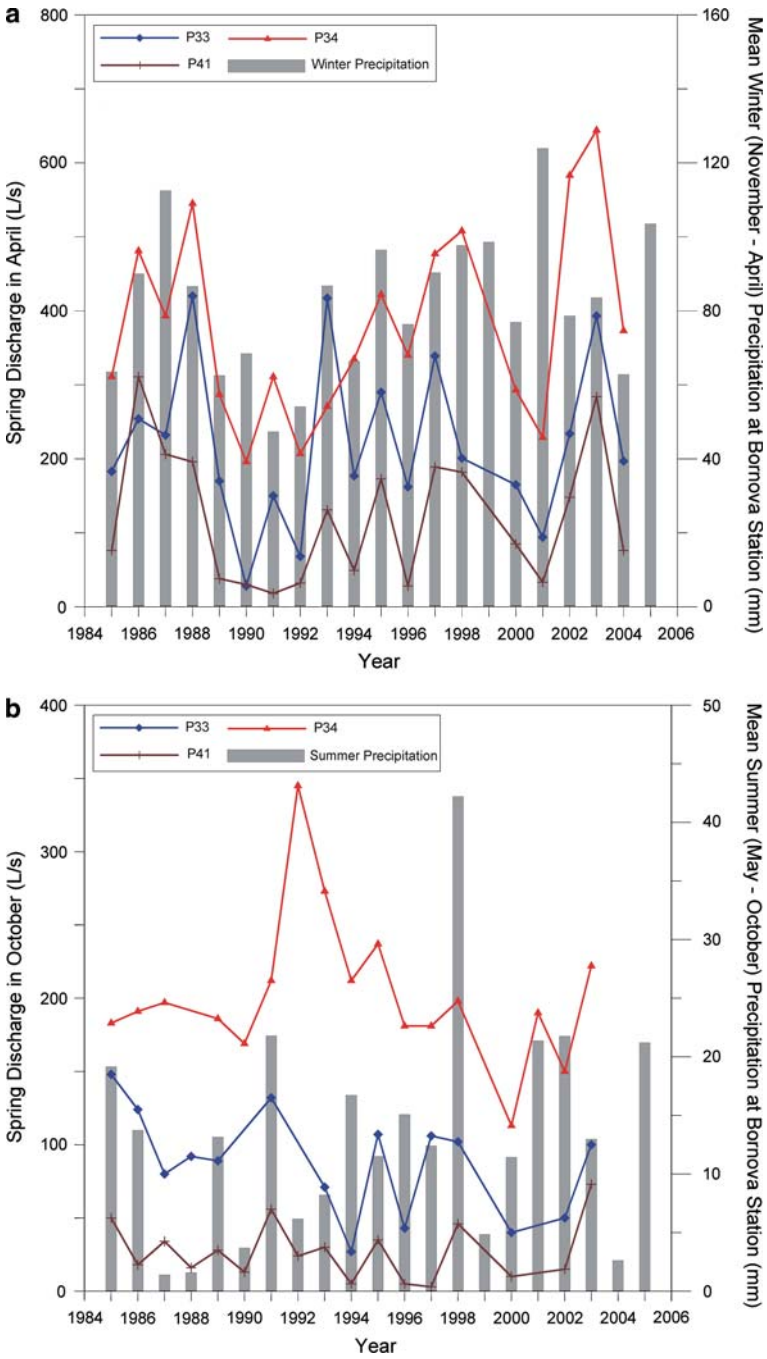

Fig. 4 Comparison of spring discharge rates and **a** wet-season and **b** dry-season averages of precipitation for the period of 1985—2005

between the sampled water and the mean global meteoric water was also calculated (IAEA 2002; Charideh and Rahman 2006). Accordingly, it has been found that the water samples collected from the study area had a deuterium excess between 3.98 and 8.87‰. Furthermore, the relation between altitude and deuterium excess was analyzed, and a positive correlation ($r = 0.61$) was found. This correlation was called the ''pseudo altitude'' by Fritz et al. (1987) and Rindsberg et al. (1990). Nevertheless, it must also be mentioned that the deuterium excess not only depends on the local topography but is also a function of the isotopic composition of precipitation water.

For the same set of samples, tritium analysis was performed to determine the age of the groundwater. It is known that tritium is an unstable isotope of hydrogen with a half-life of 12.3 years. Furthermore, as it was first released into the atmosphere after a series of nuclear tests dating back to 1953, groundwater with tritium values of less than 2 to 4 TU dates to a time before 1953. Thus, if the tritium amount in a sample is greater than this threshold, it

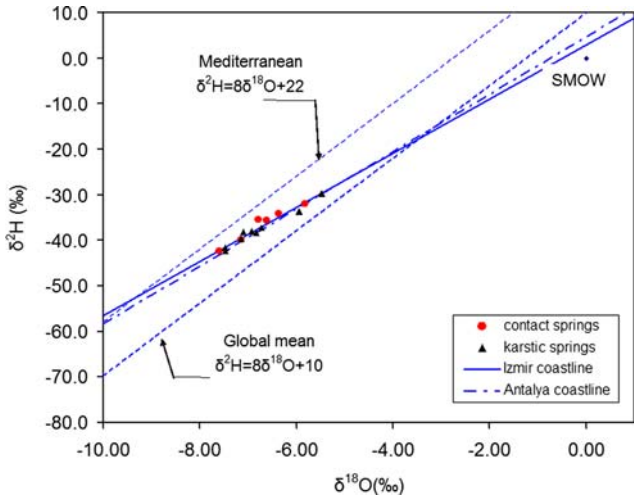

Fig. 5 Relationship between $\delta^{18}0$ and $\delta^{2}H$ values for sampled spring water

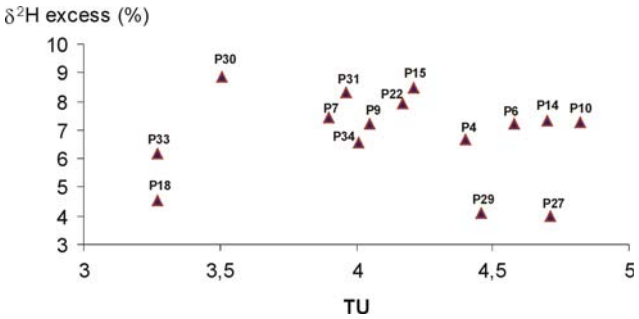

Fig. 6 Relationship between tritium and $\delta^{2}H$ excess

is considered to have been in contact with the atmosphere since 1953, and it can be concluded that the groundwater age is younger than 50 years (Fetter 2001).

The relation between tritium and deuterium excess is shown in Fig. 6, which reveals that the groundwater resources of Nif Mountain are recharged from different elevations and reach the surface from different flow paths primarily following the NE-SW general drainage pattern. Based on the analysis results, it can be concluded that the springs given in Table 1 have different circulation times. As seen from the table, the tritium values range from 3.27–3.96 TU for P-7, P-18, P-30, P-31 and P-32, all of which occur at the contact zones of two different geologic layers. On the other hand, the water samples from karstic springs P-4, P-6, P-9, P-10, P-14, and P-15 have tritium concentrations ranging from 4.05–4.82 TU, which clearly indicates that these springs have shorter circulation times compared to the contact springs. Furthermore, the water samples from two major springs in the south of the study area (P-33 and P-34) have distinctly different tritium concentrations of 3.27 and 4.01 TU, respectively. It is noteworthy that these springs are only about 2.5 km apart. Moreover, P-34, the spring in the study area with the highest recorded discharge rate during the sampling period, 877.5 L/s, has a fairly short circulation time. The travel and circulation times for P-33 are probably longer, which further implies distinct differences in permeability values for both springs.

The spring with the shortest circulation time indicated by the second highest tritium value is located to the east of the mountain and is called the Visneli spring, P-14. This spring is a typical karstic spring in the form of an open-conduit gravity spring where groundwater emerges from an open cave mouth. It also has a relatively high discharge rate of 256 L/s. Another spring in the east, P-15, is of the same type, and its water has a tritium concentration of 4.21 TU. Tritium analyses demonstrate clearly that springs originating from contact zones have longer circulation times compared to the high-discharge-rate karstic springs in the same area.

Hydrogeochemical characteristics

The chemical analysis results and the statistical overview of the water samples from the Nif Mountain karstic system are presented in Tables 2 and 3. The range of pH values for all samples is 6.46–7.93, indicating neutral to weak alkaline waters. The temperature values range from 8.7–22.6°C, with the spring samples being more at the lower end of this range. The electrical conductivity values have a broader range that varies from 212–1,583 μS/cm. With the exception of P-3 and P-5, the conductivity values of springs are below 900 μS/cm, which is within the drinking-water quality criteria. When the correlation of elevation with electrical conductivity values was evaluated (Fig. 7), it was seen that the conductivity of samples was lower at higher elevations of the mountain and increased in a nonlinear fashion as one travels towards the plains. This ''elevation'' effect is typical for areas like Nif Mountain where the levels of anthropogenic activities and rock-water interactions (i.e., shale, ophiolites and clays) increase as groundwater travels down from the uplands. This trend is also observed in hardness values of water samples to a certain extent. The hardness values range from 28.2–662.8 mg/L $CaCO_3$, with mean and standard deviation of 348.41 ± 137.22 mg/L $CaCO_3$. The high standard deviation indicates a fairly wide distribution of data points.

A Piper diagram summarizing major cation and anion concentrations is shown in Fig. 8. According to this diagram, all water samples taken from springs and wells can be characterized as Ca-HCO_3 type waters, with the exception of wells K-7 and K-19, which are of the Na-HCO_3 type. It must be noted that these wells are drilled in a Neogene claystone aquifer. A transition of Ca-HCO3 type

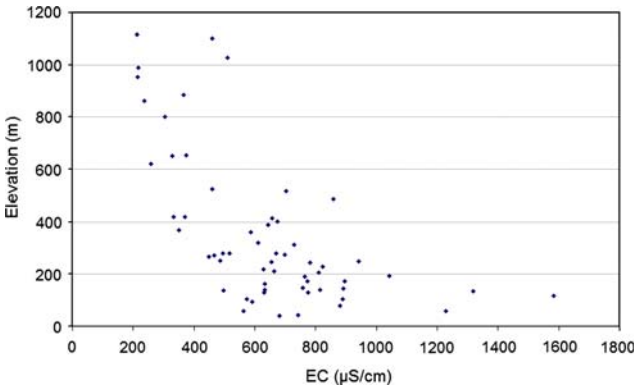

Fig. 7 Correlation of electrical conductivity with sampling elevation

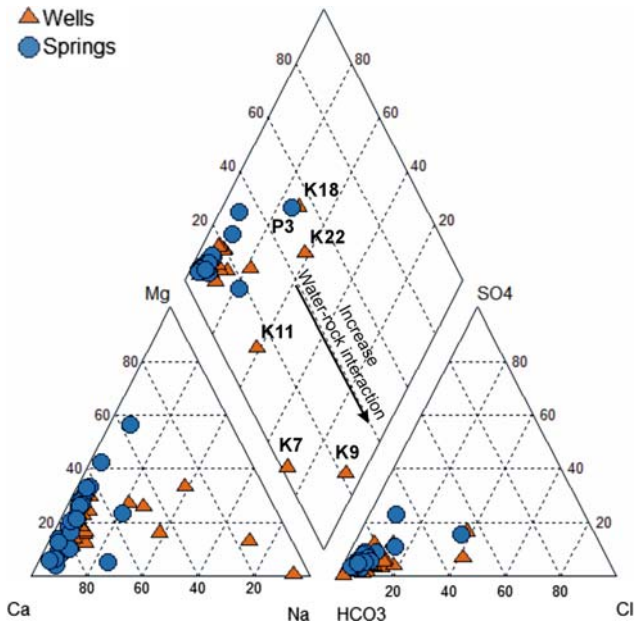

Fig. 8 The distribution of ionic composition on a Piper diagram

waters to Na-HCO_3 type waters could also be seen from the Piper diagram indicating the natural dissolution of sodium ions from Neogene claystones. In general, the sodium concentrations range from 2.5–195.2 mg/L, with an average value of 23.4 mg/L. Only the sample collected from well K-19 exceeds the drinking-water quality standard of 175 mg/L (Table 3). Calcium, magnesium and potassium concentrations range from 9.9–248, 0.9–73.6 and 0.3–22.1 mg/L, respectively. The calcium concentrations are higher than the standard value of 200 mg/L in springs P-3, P-5 and P-29. On the other hand, the magnesium concentrations exceed the standard value of 50 mg/L only in P-39. The potassium concentrations are mostly under the standard value of 12 mg/L with the exception of well K-11. In general, the concentrations of these ions are higher in Neogene aquifer systems as opposed to alluvium and karstic aquifers, which is a further indication of increased ionic strength as a direct consequence of retention time in the aquifer.

When major anions are considered, bicarbonate is the predominant ion with concentrations ranging between 133 and 719 mg/L; samples from higher altitudes resulted in higher concentrations compared to samples from the plains. Higher concentrations imply more dissolution of carbonate minerals. The presence of carbonate rocks observed in the foothills of the mountain and the general karstic structure of the region support this elevation effect. The fluoride, bromide, chloride and sulfate concentrations are typically lower compared to bicarbonate ion concentrations not exceeding 1.3, 0.5, 174.4 and 89.9 mg/L, respectively. It should also be noted that all of these maximum values are within the drinking-water quality standards currently in effect. These ions originate from the halite and ophiolite formations within flysch units.

The nitrate concentrations, on the other hand, demonstrate the opposite trend with a maximum value of 164.2 mg/L in samples collected from wells and 293.8 mg/L in samples collected from springs. It is important to note, however, that both maximums are discrete points in the data set such that when these values are excluded, the maximum nitrate concentrations become 44.3 and 32.5 mg/L in well and spring samples, respectively. Figure 9 illustrates the spatial distribution of nitrate concentrations in the study area. Highest concentrations occur in samples from Neogene series formations in the northwest of the area. Based on the fact that this area is highly residential, it could be concluded that high nitrate concentrations are mostly associated with domestic wastewater leakages from sewer lines. In this regard, the maximum nitrate of 293.8 mg/L that was observed in the P-3 spring is probably related to contamination from domestic wastewater.

To further distinguish the origin of water in the studied area, Ca/Mg, Na/Cl and Cl/Br ratios were calculated. In particular, the Ca/Mg ratio represents the carbonate and dolomite dissolutions in water, where a high Ca/Mg ratio indicates dominant limestone dissolution. It was observed that this ratio was higher for springs occurring at contact zones as opposed to high-discharge karstic springs. The means of the Ca/Mg ratio for springs and wells were 9.58 and 7.01, respectively. Moreover, the mean value of the Na/Cl ratio for the wells was 1.82, whereas for spring water it was 0.63. Interestingly, for high-discharge springs (i.e., P-14, P-15 and P-34), the Na/Cl ratio was less than 1. This result once again suggests short circulation times and therefore less chemical interaction between rock and water for these springs. The Cl/Br ratio is an indicator of the contamination mechanisms of waters in the environment (Pearson et al. 1991). The Cl/Br ratio depends not only on

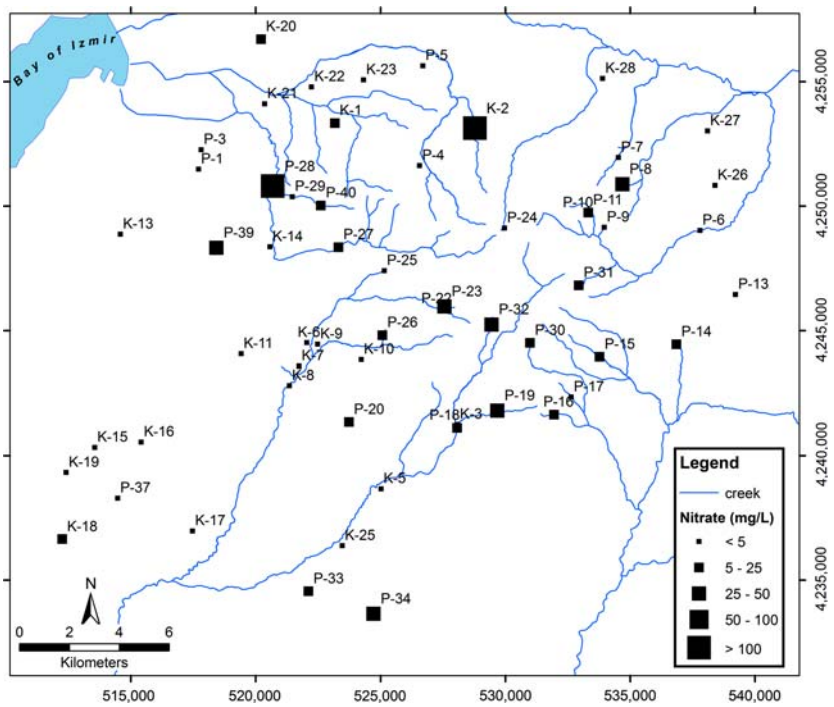

Fig. 9 The distribution of nitrate concentrations in groundwater

water-rock interactions and dissolution processes but also on environmental influences. Typically, this ratio is expected to be low for spring waters. For this study, the average Cl/Br ratio was 120.8 for wells and 68.8 for springs. High Cl/Br ratios were observed in wells drilled in the alluvial and Neogene series, which indicates that water quality is deteriorated as a function of halite and chloride dissolution from aquifer materials as well as anthropogenic activities.

Sampled water of the study area can be grouped into two categories with respect to Ca/Mg, Na/Cl and Cl/Br results: the first group represents samples from short-circuited, high-discharge karstic springs, which have less interaction with rock. The other group consists of samples taken from the aquifer in the lower plain, where interaction with minerals is longer due to slower flow velocities. The latter group comes from areas that are generally used for industrial, residential and agricultural purposes. Therefore, the chemical composition and quality of this category of water is not only determined by mineral dissolution processes, which vary for Neogene limestone and alluvial aquifers, but also by anthropogenic activities.

The analysis of major trace elements from 59 sampling points is also presented in Tables 2 and 3. Among several elements analyzed, the elements of particular interest are aluminum, arsenic and iron. Aluminum concentrations are typically under the drinking-water quality standard of 200 μg/L with the exception of K-18, where the Al concentration is 449 μg/L. This sampling point is located next to a truck parking lot and a metal processing industry, from which numerous chemicals could be released in an uncontrolled manner. As can be seen in Fig. 10, arsenic concentrations are typically under the drinking-water quality standard of TSE266 (i.e., 50 μg/L) and EPA (i.e., 10 μg/L). Only at three points (K-8, K-11 and P-39) were elevated arsenic concentrations observed. Upon a detailed analysis of these points, it was concluded that the high levels of arsenic are most probably related to local geological formations, which are likely to contain oxidized sulfite minerals in claystones. In addition, iron was found in a wide range between 10 and 434 μg/L, and it exceeded the drinking-water quality standard of 200 μg/L at two sampling points (K-10 and K-18). A positive correlation was obtained between arsenic and iron concentrations that indicates the presence of iron oxides and sulfide minerals in sedimentary rocks.

Other elements such as boron, copper, lithium and manganese were all measured to be within the drinking-water quality criteria. In particular, boron is an important parameter for irrigation water quality. It was also measured to be below the critical value of 700 μg/L (Ayers and Westcot 1985) in all but the two sampling points (K-7 and K-11) located in the Neogene-aged clay formations. Finally, zinc values given in Tables 2 and 3 also meet the drinking-water quality criteria of 3 mg/L. Although some elevated concentrations of zinc were observed in wells K-5, K-6 and K-7, they were still within the allowable range. Nevertheless, the control of this anthropogenic contami-

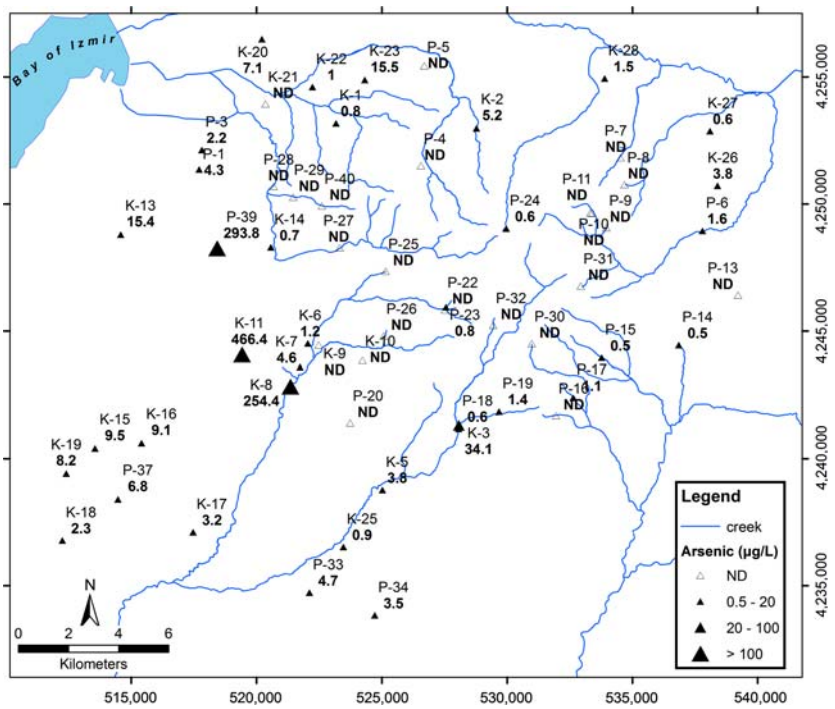

Fig. 10 The distribution of arsenic concentrations in groundwater

nant in the study area is starting to become a problem that must be monitored carefully.

Based on the hydrogeochemical characterization, it can be concluded that water originating from Nif Mountain originally has a low mineral content. As it moves towards the surrounding plains, its water quality starts to deteriorate due to natural and anthropogenic factors. This is reflected in the groundwater samples that display relatively high electrical conductivity values. The Cumaovasi plain in the southwest of the study area is under stress from small-scale industrial sites located in Menderes and Kisik, the international airport in Gaziemir, as well as the intense agricultural activities around the town of Menderes.

The spring water originating from higher elevations of the Nif Mountain can typically be classified as high-quality drinking water based on physical and chemical characteristics. Furthermore, these springs have significant water potential when the discharge values of some karstic outflows are considered. When the flow rates for the high-discharge karstic springs are taken into account, an annual water resource potential of about 50 million m^3 could be used in a sustainable manner. Taking into account several other springs for which discharge measurements could not be performed, it becomes obvious that the mentioned potential is just a lower limit of an estimation. Nevertheless, this potential represents about 28% of the mean annual inflow to the Tahtali reservoir. Thus, the natural springs of Nif Mountain have a significant potential to provide a safe supply of high-quality water for the region.

Conclusions

In this study, the Nif Mountain karstic aquifer system was characterized by using hydrogeological and hydrogeochemical methods. Being situated in a region of complex geology, the Nif Mountain and its vicinity are important for meeting water supply requirements for the Izmir metropolitan area and its surroundings. The results of this study revealed that a total of four major aquifers exist in the area, each of which has some level of hydrological interaction with Nif Mountain. From a hydrogeological point of view, the allochthonous karstic limestone aquifer is the most significant water-bearing stratum of the area. This aquifer was proven to feed a number of high-discharge springs around the mountain with pristine water quality. The wells that are drilled in this formation also provide high amounts of discharge.

In addition to the allochthonous limestone aquifer, the area has several other aquifer systems developed within the Visneli Formation such as the conglomerate aquifer, the sandstone aquifer, and the clayey-limestone aquifer, listed in a decreasing order of water supply potential. Finally, the fairly thick alluvial layers on top of these formations also demonstrate aquifer characteristics, particularly in lowland areas such as the Kemalpasa, Torbali, Bornova, and Cumaovasi plains. The isotopic and hydrogeochemical characteristics of the samples collected around the Nif Mountain area support the fact that all of these aquifer systems are strongly linked to Nif Mountain, which, in

essence, provides recharge via infiltration from surface runoff and horizontal seepage from subsurface interflow.

The springs of Nif Mountain, which originate from these aquifers, are classified into four major categories including: (1) high-discharge springs that emerge from the outcropping fractures and cracks of allochthonous limestone units, (2) high-discharge springs that emerge from the surface outcrops of conglomerate and sandstone units of Visneli Formation, (3) medium- to low-discharge springs that are formed at the contact zones of allochthonous limestone and flysch units, and (4) low-discharge springs that are formed at the contact zones of claystone and clayey-limestone units of the Visneli Formation. In particular, the high-discharge springs provide significant amounts of high-quality water and thus demonstrate potential for future use. A study by Biondic et al. (2006) provides similar insight into the relationship of spring discharge rates with the geological features of their catchment areas for a site in Slovenia.

When the quality of groundwater is considered, the results of the hydrogeochemical sampling reveal that the quality of subsurface waters deteriorated as water traveled to the plains from the uplands. This so-called elevation effect is a direct consequence of the increased levels of anthropogenic activities and rock-water interactions. Furthermore, the type of aquifer is also found to be influential on the overall quality of the water. In particular, the water quality in karstic limestone aquifers is generally better than the water quality in the aquifers of the Visneli and the alluvium aquifers. This finding is related to many factors including but not limited to the type of formation rock of the aquifer, the mean residence time of water inside the aquifer, the mean altitude of the aquifer as well as the quality and the extent of recharge that the aquifer receives.

Considering the fact that karstic limestone formations are common in the western Anatolia region, they could be utilized to provide high-quality water in large quantities, if managed in a sustainable way. It must be noted that the short-circulation characteristics of these formations make these units dependent on seasonal precipitation rates. In this regard, the results of this study show similarities with studies conducted in other parts of the eastern Mediterrenean with regards to isotopic characteristics and short circulation patterns (Charideh and Rahman 2006; Bajjali 2006). On the other hand, this study is believed to be one of the earliest examples of a hydrogeological characterization of allochthonous karstic structures buried in flysch formations.

Finally, it must also be mentioned that karstic systems are more favorable from a water quality point of view when compared to other formations if protected and maintained in a proper manner. However, they are also more vulnerable to contamination from residential, agricultural and industrial sources. This general argument is valid for the Nif Mountain karstic aquifer system where the isotopic composition and water chemistry indicate high susceptibility to contamination. Thus, recharge and discharge areas of the system must be protected from a number of future land-use practices. In particular, the land-use planning in these areas must be conducted in accordance with hydrogeological characterization such as the one presented in this study.

Acknowledgements This study was funded by the Scientific and Technological Research Council of Turkey (TUBITAK), project no. 104Y290 and the Marie Curie International Reintegration Grant MIRG-CT-2005-029133 within the 6th European Community Framework program. The authors are thankful to Yetkin Dumanoglu and Rahime Polat for their assistance in anion analyses by ion-chromatography.

References

Ayers RS, Westcot DW (1985) Water quality for agriculture. FAO irrigation and drainage paper no. 29, rev. 1. U. N. Food and Agriculture Organization, Rome

Baba A, Sozbilir H (2001) The geology and groundwater quality of the NE-directed Torbali and Kemalpasa plain, West Anatolia. Paper presented at the I. Environmental Geology Symposium (CEVJEO-2001), Izmir, 21–23 March 2001 (in Turkish)

Bajjali W (2006) Recharge mechanism and hydrochemistry evaluation of groundwater in the Nuaimeh area, Jordan, using environmental isotope technique. Hydrogeol J 14:180–191

Biondic B, Biondic R, Kapelj S (2006) Karst groundwater protection in the Kupa river catchment area and sustainable development. Environ Geol 49:828–839

Charideh A, Rahman A (2006) Environmental isotopic and hydrochemical study of water in the karst aquifer and submarine springs of the Syrian coast. Hydrogeol J. DOI:10.1007/s10040-006-0072-x

Demirkiran Z, Cetiner L, Simsek C, Gunduz O, Ocal G (2006) Interactive three-dimensional modeling and characterization of the hydrogeological structure of Kemalpasa. Paper presented at the 30th Annual Fikret Kutman Geology Symposium, 20–23 September, Konya (in Turkish)

DMI (2006) Station report (in Turkish). General Directorate of State Meteorological Service, Izmir Regional Directorate, Izmir, Turkey

Erdogan B, Gungor T (1992) The stratigraphy and tectonic evolution of the northern portions of the Menderes Massive (in Turkish). TPJD Bull C 4/1, Izmir

Fetter CW (2001) Applied hydrogeology. Prentice Hall, Upper Saddle River

Fritz P, Drimmie RJ, Frape SK, O'Shea K (1987) The isotopic composition of precipitation and groundwater in Canada. In: Proceedings of a Symposium on Isotope Techniques in Water Resources Development. IAEA, pp 539–550

Gunay G (2006) Hydrology and hydrogeology of Sakaryabasi karstic springs, Cifteler, Turkey. Environ Geol 51:229–240

Hiscock K (2005) Hydrogeology: principles and practice. Blackwell, Malden, MA

IAEA (2002) Statistical treatment of data on environmental isotopes in precipitation (period 1960–1997). Technical report series no. 331. International Atomic Energy Agency, Vienna

Inci U (1991) The facies and sedimentation conditions of the Miocene-aged terrestrial units of Northern Torbali (Izmir) (in Turkish). MTA J 112:13–26

Kacaroglu F (1999) Review of groundwater pollution and protection in karst areas. Water Air Soil Pollut 113:337–356

Pearson FL, Balderer W, Lossli BE, Lehmann BE, Matter A, Peters TJ, Schmassman H, Gautschi A (1991) Applied isotopes hydrogeology a case study in northern Switzerland. Elsevier, Amsterdam

Rindsberger M, Jaffe SH, Rahamin SH, Gat JR (1990) Patterns of isotopic composition of precipitation in time and space: data from the Israeli storm water collection program. Tellus 42B:263–271

Sen Z (1995) Applied hydrogeology for scientists and engineers. CRC Press, Boca Raton

Simsek C (2002) The hydrogeological investigations for the site selection of the landfill area of the Torbalí Plain. PhD Thesis, Graduate School of Natural and Applied Science, Dokuz Eylul University, Izmir

Sozbilir H (2000) Active faults and potentially active faults; examples from western Anatolia (in Turkish). Paper presented at the BAKSEM Symposium for West Anatolia Earthquake Studies, 24–27 May 2000, Izmir, pp 133–142

White WB (2002) Karst hydrology: recent developments and open questions. Eng Geol 65:85–105